

## REFRESHED SHOCKS and AFTERGLOW LONGEVITY in GRB

M.J. Rees<sup>1</sup> & P. Mészáros<sup>2</sup>

### ABSTRACT

We consider fireball models where the ejecta have a range of bulk Lorentz factors, so that the inner (lower  $\Gamma$ ) parts may carry most of the mass, or even most of the energy. The outer shock and contact discontinuity decelerate as the fireball sweeps up external matter. This deceleration allows slower ejecta to catch up, replenishing and reenergizing the reverse shock and boosting the momentum in the blast wave. In consequence, the energy available to power the afterglow may substantially exceed that of the burst itself. Such models allow a wide range of possibilities for the afterglow evolution, even in the case of spherically symmetric expansion.

*Subject headings:* gamma-rays: bursts

### 1. Introduction

Afterglows from Gamma-Ray Bursts (GRB) have been discovered in at least seven objects at X-rays wavelengths. Two of these also yielded optical afterglows and one was followed in up to the radio band (e.g. papers at the 4th Huntsville GRB Symposium, Meegan et al, 1997). The first afterglow discovered at both X-ray and optical wavelengths, GRB 970228 (Costa et al, 1997) strongly favored a cosmological origin, and this was strengthened even further by the discovery in the second object, GRB 970508, of several systems of absorption lines yielding a limit  $0.835 \lesssim z \lesssim 2.3$  (Metzger et al, 1997). The power law flux decay predicted from the simplest cosmological fireball afterglow model (Mészáros & Rees, 1997) turned out to be in good general agreement with the observed behavior (e.g. Tavani, 1997; Waxman, 1997a; Vietri, 1997b; Wijers, Rees & Mészáros, 1997; Reichart, 1997). The simple model is also successful in explaining the rise and decay of the light curves (Wijers, Rees & Mészáros, 1997), as well as the overall radio behavior (Goodman, J., 1997; Waxman, et al, 1997c). The ensuing massive observational campaigns on these sources have, in the meantime, provided such excellent data that it is now

---

<sup>1</sup>Institute of Astronomy, Cambridge University, Madingley Road, Cambridge CB3 0HA, U.K.

<sup>2</sup>Dpt. of Astronomy & Astrophysics, Pennsylvania State University, University Park, PA 16803

feasible to investigate more subtle effects. Among these are, e.g. possible oscillations superposed on the power law decay (e.g. Galama, et al., 1997), the appearance of optical and X-ray bumps after  $\sim 1.5$  days on the optical and X-ray light curves (Piro, et al, 1997), the evidence for an initial slow optical decay before the onset of the power law rise and decay (Pedersen, et al, 1997), etc. Most and perhaps all of these features may be understood within the context of anisotropic outflows, or of isotropic outflows in inhomogeneous media (Mészáros, Rees & Wijers 1997). It remains, however, an interesting question to investigate how slow can a power law decay behavior be in a simple spherically symmetric model, and what fraction of the total energy budget can be associated with the late afterglow, as opposed to the initial GRB. In most earlier discussions, the ejecta have been treated as a uniform sphere or shell, where most of the energy is carried by material with a well-defined (and generally high) Lorentz factor. But it is possible – perhaps, indeed, more physically realistic – that the ejecta consist, in effect, of many concentric shells moving at different (relativistic) speeds. This could be the outcome, for instance, of relativistic shock propagation down a density gradient; or the inner shells might be more heavily loaded with baryonic ejecta. A given shell would then expand freely until the contact discontinuity had been decelerated, by sweeping up external material, to a Lorentz factor lower than its own. It would then crash into a reverse shock, thermalizing its energy and boosting the power of the afterglow. In this paper, we illustrate this phenomenon by discussing simple cases. We show that such models can produce very slow decay rates in the afterglow; they can accommodate very large (as well as small) ratios of afterglow to burst fluences, and can naturally explain a variety of afterglow light curves.

## 2. Kinematics of Ejecta with a Power-Law Radial Profile

The ‘trigger’ for a gamma ray burst may have complex time structure spread over the duration (typically 10 seconds) of the intense gamma ray emission itself. However, when we are considering mechanisms for the (much more prolonged) afterglow, we can treat this energy release as impulsive. It gives rise to relativistically expanding debris which eventually slows down as it sweeps up external matter. If the debris were spherical, it would be characterized by the way its energy and mass were distributed among shells of different Lorentz factor. The actual ‘ $\Gamma$ -profile’ would be the outcome of complex dynamics during the burst itself: shock fronts propagating down density gradients, internal shocks, etc. A range of Lorentz factors seems likely – indeed it is not obvious whether the energy (or even the mass) would be concentrated towards the high or low end of the  $\Gamma$  distribution. This is our motivation for first exploring a range of power-law’ models, which can be treated analytically. In simple cases where the expansion is ultrarelativistic (bulk Lorentz factor  $\Gamma \gg 1$ ) and all physical variables depend as power laws on radius (or source-frame time), the dynamics can be treated in a 1-D approximation, which will be valid either for spherical expansion or for jet angles  $\gtrsim \Gamma^{-1}$ . We consider the evolution at large radii, after the input of mass and energy from the central source has ceased. In the source frame, after deceleration by the external medium becomes important, the Lorentz factor of the outer shock and the contact

discontinuity begin to decrease as

$$\Gamma_c \propto r^{-n}, \quad (1)$$

When the ejecta have, in effect, a single (high) Lorentz factor, we have the well-known models where  $n = 3/2$  for adiabatic (weak coupling), or  $n = 3$  for radiative (strong coupling) expansion in a homogeneous external medium (for an inhomogeneous medium, see Mészáros, Rees & Wijers, 1997). In the cases treated here, where the ejecta has a range of Lorentz factors  $\Gamma_f$ , the expansion will still obey a power law, but with different  $n$ . At increasing  $r$  the contact discontinuity, if it expands according to (1), lags behind the light cone by a fractional amount

$$\frac{\Delta r}{r} \propto \frac{1}{2r} \int \Gamma_c^{-2}(r) dr \propto \frac{1}{2r} \int^r r^{-2n} dr \propto \frac{1}{2(2n+1)} \Gamma_c^{-2}(r). \quad (2)$$

We assume that the input of energy is variable, but occurs over a finite time which is short compared to the deceleration time of the contact discontinuity, so the impulsive approximation is valid. Subsequent shells of fireball material endowed with a decreasing Lorentz factor  $\Gamma_f$ , catch up with the contact discontinuity at radii  $r$  which satisfy  $(\Delta r/r) = [2(2n+1)]^{-1} \Gamma_c^{-2} = (1/2) \Gamma_f^{-2}$ , or

$$\Gamma_f(r) = (2n+1)^{1/2} \Gamma_c(r), \quad (3)$$

where we have neglected the thickness of the shell of reverse shocked gas relative to  $r$ . This is shown in Figure 1, where  $r$  is distance from the center of the outflow and  $t$  is source-frame (not detector) time,  $t = r/c$ . The impacting material therefore has a Lorentz factor which is  $(2n+1)^{1/2}$  times larger than that of the contact discontinuity. (The latter has been decelerated, whereas the former, having moved at constant speed, reaches the same radius with a higher speed, see Figure 1). The ratio of the Lorentz factors, however, is only a factor  $\sim 2$ , so the reverse shock(s) are marginally relativistic at all times. It then makes little difference to the overall dynamics whether the shock is radiative or adiabatic.

### 3. Effects of a $\Gamma_f$ -dependent Mass and Energy Input

We assume that the primary event leading to the GRB produces a fireball in which the mass fraction ejected above a given initial bulk Lorentz factor decreases according to

$$M(\geq \Gamma_f) \propto \Gamma_f^{-s}. \quad (4)$$

The mass is dominated by the low  $\Gamma_f$  shells for  $s > 0$ , while the energy will also be dominated by low  $\Gamma_f$  material if  $s > 1$ . The mass that has 'caught up' with the contact discontinuity, and passed through the reverse shock, before it gets out to radius  $r$  is (assuming  $\Delta r/r \ll 1$ )

$$M(< r) \propto r^{ns} \quad (5)$$

The momentum impacting on the contact discontinuity from the reverse shocked gas, per unit solid angle and measured in the comoving frame, is

$$p_{rev} \propto \frac{dM(< r)}{dr} \propto r^{ns-1}. \quad (6)$$

The impact is always marginally relativistic,  $\Gamma_{rev} \sim 2 \sim \text{constant}$ . The force on the other (forward shock) side of the contact discontinuity is

$$p_{for} \propto \rho_{ext} \Gamma_c^{1+A} r^2, \quad (7)$$

where  $A = 0$  for radiative (strong coupling) and  $A = 1$  for adiabatic (weak coupling) expansion of the remnant (Mészáros, Rees & Wijers, 1997), and the geometrical factor  $r^2$  is included because this is per unit solid angle. Here the adiabatic or radiative dependence is important, since the outer shock is ultrarelativistic. We note that  $A = 0$  and  $A = 1$  are extremes of the remnant behavior; intermediate values are also expected in realistic cases, e.g., as shown in the numerical calculations of Panaitescu & Mészáros, 1997. For  $\rho_{ext}$  independent of radius, equating the powers of  $r$  in equations (6) and (7) gives  $ns - 1 = -n(1 + A) + 2$ , so the index  $n = 3/(s + 1 + A)$  and the radius dependence of the contact discontinuity Lorentz factor in the presence of a continuous input of mass and energy is

$$\Gamma_c \propto r^{-n} \propto r^{-3/(s+1+A)}. \quad (8)$$

The value of this index is shown in Table 1 for various cases.

We see that, for  $s = 0$  (where the later arriving, slower mass makes only a logarithmic difference to the total), we recover as expected the previous law of  $n = 3/2(3)$  for the  $A = 0(1)$  cases corresponding to the adiabatic (radiative) dynamic regimes. However for  $s = 1$ , where most of the mass is concentrated at lower  $\Gamma_f$  we get  $n = 1(3/2)$  for  $A = 0(1)$ ; and for  $s = 3/2$ , where also most of the energy is dominated by the low  $\Gamma_f$ , we get  $n = 6/7(6/5)$  for  $A = 0(1)$ .

#### 4. Luminosity and Flux Evolution

For  $s > 1$  the total energy available for the afterglow gradually increases during the deceleration, but clearly the power law dependences will only be valid over a finite range of times. Keeping these limitations in mind, the luminosity dependence at late times can be evaluated. For a contact discontinuity evolution given by equation (8), the energy liberated by the shock is  $E \propto \Gamma_c^{1-s} \propto r^{-3(1-s)/(s+1+A)}$  and the observer time over which this is released is  $T \propto r/\Gamma_c^2 \propto r^{(s+A+7)/(s+1+A)}$ , corresponding to  $r \propto T^{(s+1+A)/(s+A+7)}$ . The “kinetic” luminosity or flux is then

$$F_{kin} \propto r^{-(10-2s+A)/(s+1+A)} \propto T^{-(10-2s+A)/(7+s+A)}. \quad (9)$$

where  $T$  is detector (observer-frame) time. E.g., for  $s = 3/2$ ,  $A = 1$  we have  $F_{kin} \propto T^{-16/19}$ .

If the radiation comes from the forward shock, and is due to synchrotron radiation of shock-accelerated power law electrons in a turbulently generated magnetic field which has built up to some fraction of equipartition with the protons, we have a comoving synchrotron peak frequency  $\nu'_m \propto \gamma_e^2 B' \propto \Gamma_c^3 \propto r^{-9/(s+1+A)} \propto T^{-9/(s+A+7)}$ , and the corresponding observer-frame value is  $\nu_m \propto \Gamma_c \nu'_m \propto T^{-12/(s+A+7)}$ , where  $\gamma_e$  is the electron random Lorentz factor. Following Mészáros, Rees & Wijers 1997 the comoving synchrotron peak intensity is  $I'_{\nu'_m} \propto n'_e \gamma_e \nu'^{-1}_m e_{sy}$ ,

where  $n'_e \propto \Gamma_c n_{ext} \sim \Gamma_c$  is the comoving postshock electron density for expansion in a homogeneous external medium, and  $e_{sy} \propto (t'_{dyn}/t'_{sy})^a \propto r^a \Gamma_c^{2a}$  is the synchrotron radiative efficiency of the electrons responsible for radiating at the peak frequency. For  $a = 0$  the electrons are radiatively efficient and  $e_{sy} = 1$ , while for  $a = 1$  the electrons are adiabatic (radiatively inefficient) and  $e_{sy} < 1$ . Thus  $I'_{\nu'_m} \propto r^a \Gamma_c^{2a-1} \propto T^{[a(s+1+A)-6a+3]/(s+A+7)}$ . The observer frame peak synchrotron flux is

$$F_{\nu_m} \propto T^2 \Gamma_c^5 I'_{\nu'_m} \propto T^{-[6a-(s+1+A)(2+a)]/(s+A+7)} \quad (10)$$

For a synchrotron intensity spectral slope  $\beta$  above the synchrotron peak,  $I_\nu \propto \nu^\beta$ , the time decay of the flux in a fixed detector frequency band  $\nu_D$  (e.g. optical) is

$$F_D \propto F_{\nu_m} (\nu_D/\nu_m)^\beta \propto T^{[(2+a)(s+1+A)-6a+12\beta]/(s+A+7)} \quad (11)$$

For  $s = 3/2$ ,  $A = 1$  this is  $\propto T^{[7-(5a/2)+12\beta]/(19/2)}$  and for  $a = 1$ ,  $\beta = 1/3$  (e.g. synchrotron radiation below the peak from adiabatic electrons) the flux would increase  $\propto T^{17/19}$ , steeper than in our previous models. For  $a = 1$ ,  $\beta = -1$  (above the peak) the flux is  $\propto T^{-15/19}$ . Similar considerations can be made for the reverse shock; however, if Rayleigh-Taylor instabilities occur across the contact discontinuity (e.g. Waxman & Piran, 1994), these would tend to equalize the magnetic and nonthermal energy densities, leading to a similar time-dependence of the emission. Further complications may arise if the electrons responsible for  $\nu_m$  are adiabatic but those responsible for  $\nu_D$  are radiative, e.g. equation (9) in Mészáros, Rees & Wijers 1997 and related discussion (also Sari, Piran & Narayan, 1997). Note that equation (11) above was calculated assuming  $\beta \lesssim -1$ . For  $\beta \gtrsim -1$  most of the energy does not reside at  $\nu_m$  but at some largest frequency  $\nu_{cut}$  to which the slope  $\beta$  extends to, and the equation replacing (11) would depend on this cutoff frequency. The cutoff can be computed, given model hypotheses defining the absolute values of the magnetic field and  $\Gamma_c$ . Note also that equations (8,9,10, 11) can be easily generalized to take into account a dependence on an external medium that depends on radius as  $n_{ext} \propto r^{-d}$ , as in Mészáros, Rees & Wijers 1997, leading to flatter decay laws than in equation (11). In Table 1 we show the values of the time exponents of the fluxes in a fixed detector band for a homogeneous external medium and some representative values of  $s$ ,  $A$ ,  $a$  and  $\beta$ .

## 5. Discussion

We have considered here GRB models where the fireball does not constitute a single ultrarelativistic shell (or uniform sphere), but contains material with a range of speeds, larger amounts of mass and energy being characterized by lower bulk Lorentz factors. After the central energy-generation has ceased the impulsive approximation is valid, and during its evolution the later portions of the ejecta catch up with the previously decelerated matter, thus continually re-energizing the shock that provides the afterglow of the GRB. We have shown in §4 that, depending on the Lorentz factor dependence of the mass and energy injection, even spherically symmetric outflows can produce very flat flux time decay laws (equations [11]). Even flatter

decay laws are possible for synchrotron energy spectral indices  $\beta \gtrsim -1$ . A significant departure from our previous versions of an isotropic GRB afterglow model is that here the flux decay law is not dependent only on the spectral index (or on the density or angular dependence indices, c.f. Mészáros, Rees & Wijers, 1997) but also on the index  $s$  of the Lorentz factor dependence of the mass and energy ejection (equation [4]). Even for a homogeneous medium and for isotropic outflow, plausible values of  $s$  can lead to afterglow luminosities whose time-integrated value can either exceed or fall below the initial  $\gamma$ -ray fluence. The former case would represent a situation similar to the hypernova model of Paczyński, 1997.

Although we have focused on power-law dependences (cf equation (1) and (4)), our considerations clearly show that even a spherical model could generate more complicated light curves. For example, suppose that, rather than containing material with a smooth distribution of  $\Gamma_f$ , the fireball could be better modeled by two shells with very different  $\Gamma_f$ , the slower shell carrying more energy. The afterglow luminosity would initially decline as in the standard mono-energetic case; but when the blast wave had slowed down enough for the slower shell to catch up, there would be a boost to the luminosity before it again resumed a power-law decline. Changes in the slope of the flux decay laws (equations [11]), or late bumps (e.g. Piro et al, 1997), could thus be readily incorporated even into spherical models. The “internal engine” associated with a catastrophic disruption or collapse event would inevitably lead to non-sphericity in the outflow; if the ejecta consisted of discrete overdense blobs, their deceleration could lead to more complex time-structure, or apparent shorter-term variability (Galama et al, 1997, Pedersen, et al, 1997) superposed on the overall power law behavior.

This research has been supported by the Royal Society, NASA NAG5-2857 and NATO CRG-931446. We are grateful to A. Panaitescu and R.A.M.J. Wijers for valuable comments.

## REFERENCES

- Costa, E, et al., 1997s, *Nature*, 387, 783
- Galama, T., et al., 1997, *Nature* 387, 479
- Goodman, J., 1997, *New Astronomy*, 2(5), 449
- Meegan, C, Preece, R and Koshut, T, 1997, eds, *4th Huntsville GRB Symposium*, (New York: AIP), in press.
- Mészáros, P & Rees, M.J., 1997a, *ApJ*, 476, 232
- Mészáros, P, Rees, M.J. & Wijers, R.A.M.J., 1997, *ApJ*, in press (astro-ph/9709273)
- Metzger, M et al., 1997, *Nature*, 387, 878

- Paczynski, B., 1997, ApJ, in press (astro-ph/9710086)
- Panaitescu, A. & Mészáros, P., 1997, ApJ, subm (astro-ph/9711339) (astro-ph/9710086)
- Pedersen, H., 1997, preprint (astro-ph/9710322)
- Piro, L., et al, 1997, preprint (astro-ph/9710355)
- Reichart, D., 1997, ApJ, in press (astro-ph/9704198)
- Sari, R., Piran, T. & Narayan, R., 1997, ApJ, subm (astro-ph/9712005)
- Tavani, M., 1997, ApJ, 483, L87
- Vietri, M., 1997b, ApJ, subm (astro-ph/9706060)
- Waxman, E. & Piran, T., 1994, ApJ, 433, L85
- Waxman, E., 1997a, ApJ, subm (astro-ph/9704116)
- Waxman, E., Kulkarni, S. & Frail, D., 1997c, ApJ, subm (astro-ph/9709199)
- Wijers, R.A.M.J., Rees, M.J. & Mészáros, P., 1997, MNRAS, 288, L51

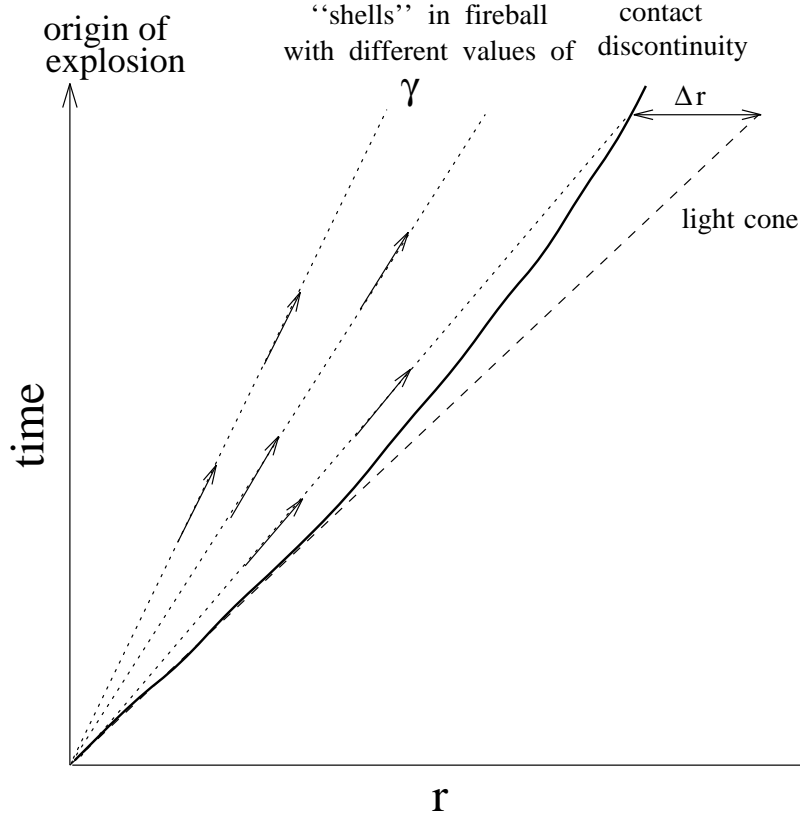


Fig. 1.— Schematic space-time diagram in source frame coordinates of a relativistic outflow, with a range of Lorentz factors  $\Gamma_f$ , triggered by an explosion that can be approximated as instantaneous (decreasing  $\Gamma_f$  values lead to world lines further to the left, which are straight before entering the shock). The contact discontinuity and the forward shock are being decelerated due to the increasing amount of external matter being swept up, so that they lag behind the light cone by an increasing amount amount  $\Delta r$  whose increase with  $r$  is steeper than linear. This deceleration allows slower ejecta (with lower  $\Gamma_f$ ) to catch up and pass through a reverse shock just inside the contact discontinuity. Both shocks are here approximated as having negligible width. Energy and momentum from progressively slower material is thus continuously re-energizing the shocks, resulting in a more gradual decay of the afterglow.

A	s	n	a	$F_{kin}$	$F_D$	$F_D$	$F_D$
				$\beta = 1/3$	$\beta = -1$	$\beta = -3/2$	
0	0	3/2	0	-10/7	6/7	-10/7	-16/7
0	1	1	0	-1	1	-1	-14/8
0	3/2	6/7	0	-14/17	18/17	-14/17	-26/17
1	0	3	0	-11/8	1	-1	-14/8
1	1	3/2	0	-1	10/9	-2/3	-12/9
1	3/2	6/5	0	-16/19	22/19	-10/19	-22/19
1	0	3	1	-11/8	1/2	-12/8	-18/8
1	1	3/2	1	-1	7/9	-1	-15/9
1	3/2	6/5	1	-16/19	17/19	-15/19	-27/19

Table 1: For strong coupling (“radiative”,  $A = 0$ ) or weak coupling (“adiabatic”,  $A = 1$ ) remnant evolution in a homogeneous external medium and a mass outflow index  $s$  ( $M(\geq \Gamma_f) \propto \Gamma_f^{-s}$ ) the bulk Lorentz of the contact discontinuity evolves as  $\Gamma_c \propto r^{-n}$ , producing a kinetic flux  $F_{kin} \propto t^v$  whose index  $v$  is in column 5. For different spectral indices  $\beta$  the forward shock produces a flux in a fixed detector band  $F_D \propto t^w$ , whose indices  $w$  are shown in columns 6 through 8 for radiative ( $a = 0$ ) or adiabatic ( $a = 1$ ) electrons. Flatter decay laws would be obtained if the external density decreases with radius.